Inelastic scattering of electrons in solids from a generalized oscillator strength model using optical and photoelectric data

1993 J. Phys.: Condens. Matter 5 3593

(http://iopscience.iop.org/0953-8984/5/22/011)

J. Phys.: Condens. Matter 5 (1993) 3593–3610. Printed in the UK

Inelastic scattering of electrons in solids from a generalized oscillator strength model using optical and photoelectric data

J M Fernández-Varea†, R Mayol†, D Liljequist‡ and F Salvat†

† Facultat de Física (ECM), Universitat de Barcelona, Societat Catalana de Física (IEC), Diagonal 647, 08028 Barcelona, Spain

‡ Department of Physics, University of Stockholm, Vanadisv. 9, S-113 46 Stockholm, Sweden

Received 30 September 1992

Abstract. Inelastic scattering of electrons in solids is computed from a generalized oscillator strength model based on optical and photoelectric data. The optical oscillator strength is extended into the non-zero momentum transfer region by using free-electron gas dispersion for the weakly bound electrons. The applicability of this method to non-conduction valence electrons and to inner shells is discussed. A different extension method, which reproduces ionization thresholds, is used for inner-shell ionization. The calculations are simplified by using a two-modes model for the Lindhard theory of the free-electron gas. Exchange effects are accounted for by means of a modified Ochkur approximation. Inelastic mean free paths and stopping powers obtained from this optical-data model for four materials (Al, Si, Cu and Au) and for electrons with energies from 10 eV to 10 keV are presented.

1. Introduction

During the past few years, a number of phenomenological 'optical-data' models to compute the inelastic scattering of electrons in solids have been proposed. The common characteristic of these models is the use of an optical oscillator strength (OOS) obtained from experimental optical data, which is extended into the non-zero momentum transfer region by means of a physically motivated (but in general approximate) relation between momentum transfer and energy transfer, subsequently referred to as the 'extension algorithm'. In the simplest versions, this relation may be a dispersion formula giving energy transfer as a single-valued function of momentum transfer. In this way, a model of the generalized oscillator strength (GOS) is obtained.

A predecessor of the optical-data model calculations is the work of Tung *et al* [1], who used the OOS obtained from the local plasma approximation [2] and extended it into the GOS by means of the Lindhard theory for the homogeneous free-electron gas (FEG) [3]. The first calculations based on experimental OOSs were performed by Ashley [4] (see also [5, 6]) using a one-mode approximation instead of the Lindhard theory in order to simplify the numerical calculations. More recently, Penn [7] proposed a similar model in which the GOS is obtained by extending the experimental OOS by means of the Lindhard theory. The extension algorithms based on FEG theory appear to be adequate to describe excitations of weakly bound electrons. However, they fail to account properly for inner-shell ionizations. An extension algorithm more suited for this has been investigated by Mayol and Salvat [8]. In a previous paper [9] we have presented a comparative study of some different GOS models.

0953-8984/93/223593+18$07.50

The optical-data models are typically used to describe inelastic scattering of electrons with kinetic energies from $\sim$ 10 eV up to $\sim$ 10 keV. It may be noted that, while the differential cross section (DCS) for the most probable excitations (i.e. those involving low momentum transfers, which correspond to small scattering angles) is almost completely determined by the OOS, a model of the GOS is required for the calculation of the complete DCS, the inelastic mean free path and the stopping power. It should also be noted that exchange effects have a non-negligible influence on the scattering process [5], even for high-energy electrons. Energies higher than a few tens of keV require the introduction of relativistic corrections (see e.g. [8]).

In the present paper we propose a new optical-data GOS model for calculating inelastic DCSs for electrons in solids. The model is designed to serve also as a suitable basis for sampling routines in a Monte Carlo simulation. In summary, our method is as follows. The information needed to compute the DCS is provided by the OOS. Excitations of weakly bound electrons are treated by using FEG theory as the extension algorithm. A two-modes model of the Lindhard FEG theory is used to simplify the calculations. Inner-shell ionizations are treated by means of the alternative extension algorithm used in [8]. Exchange effects are introduced through a modified Ochkur approximation [10, 11] which leads to the non-relativistic Møller DCS for binary electron collisions.

Inelastic mean free paths and stopping powers have been computed for electrons with kinetic energies in the range 10 eV to 10 keV and for four single-element materials, for which OOSs are available from the literature. Fitted analytical formulae for these quantities are also given.

2. Theory

2.1. Basic relations

Inelastic interactions of non-relativistic electrons having velocity v with isolated atoms or molecules can be described, to the first-order Born approximation, by means of the DCS [12]

$$\mathrm{d}^2\sigma/\mathrm{d}Q\mathrm{d}W = (\pi e^4/E)(1/WQ)(\mathrm{d}f(Q,W)/\mathrm{d}W) \tag{1}$$

where e is the electron charge, $E = \frac{1}{2}mv^2$, W is the energy transfer and Q, which for brevity is named the 'recoil energy', is defined as

$$Q = q^2/2m \tag{2a}$$

where q is the momentum transfer and m is the electron mass. Q is related to the scattering angle θ by

$$Q = 2E - W - 2[E(E-W)]^{1/2}\cos\theta. \tag{2b}$$

The quantity $\mathrm{d}f(Q,W)/\mathrm{d}W$ is the GOS, which completely characterizes the target (within the Born approximation) [12]. It satisfies the Bethe sum rule [12, 13]

$$\int_0^\infty \frac{\mathrm{d}f(Q,W)}{\mathrm{d}W}\,\mathrm{d}W = Z \tag{3}$$

where Z is the number of electrons per atom or molecule.

For condensed media, the usual approach is to start from the dielectric energy-loss function $\mathrm{Im}[-1/\epsilon(Q, W)]$, which is related to the GOS through [14]

$$\mathrm{d}f(Q, W)/\mathrm{d}W = (2W/\pi\Omega_p^2)Z\,\mathrm{Im}\,(-1/\epsilon(Q, W)) \tag{4}$$

where $\epsilon(Q, W)$ is the dielectric function of the stopping material. Ω_p is given by

$$\Omega_p = (4\pi\hbar^2 e^2 N Z/m)^{1/2} \tag{5}$$

where N is the number of atoms or molecules per unit volume. Ω_p coincides with the plasmon energy of an homogeneous electron gas with a density equal to the average electron density of the stopping material. Using equation (4), the GOS concept and equation (1) can be applied to inelastic scattering in condensed matter and in the homogeneous electron gas. In the latter case, it is more convenient to refer to the 'one-electron GOS' (GOS per electron), i.e. the Bethe sum rule (3) for the electron gas adds to unity. Equation (1) (with equation (4)) has been applied with some success down to energies of about 10 eV [1, 4–7], in spite of the fact that the Born approximation and the description of the electron as being scattered between plane-wave states appears doubtful at these energies.

The inelastic mean free path λ and the stopping power S are given by

$$\lambda^{-1} = N\sigma^{(0)} \qquad S = N\sigma^{(1)} \tag{6}$$

where $\sigma^{(0)}$ and $\sigma^{(1)}$ are the total inelastic cross section and the stopping cross section, respectively, defined by

$$\sigma^{(n)} \equiv \int_0^{W_{max}} \mathrm{d}W\, W^n \int_{Q_-}^{Q_+} \mathrm{d}Q\, \frac{\mathrm{d}^2\sigma}{\mathrm{d}Q\mathrm{d}W}. \tag{7}$$

If we, for the moment, neglect exchange, the maximum energy loss is $W_{max}=E$. For a given W and varying scattering angle, the kinematically allowed recoil energies lie in the interval $Q_- < Q < Q_+$ given by

$$Q_\pm = [E^{1/2} \pm (E - W)^{1/2}]^2. \tag{8}$$

The GOS is known analytically only for the simplest atomic target, namely the hydrogen atom (see e.g. [12]). The dielectric function of the FEG, derived from the random phase approximation, has been given in analytical form by Lindhard [3]. The GOS for inner shells in certain atoms has been computed, for example by Leapman *et al* [15]. Except for certain cases such as Al [16], the complete GOS has not been calculated from first principles; it also seems to be, in general, a formidable task.

In the optical limit, $Q = 0$, the GOS reduces to the OOS, $\mathrm{d}f(W)/\mathrm{d}W \equiv \mathrm{d}f(0, W)/\mathrm{d}W$. It should, however, be observed that, as regards inelastic scattering in condensed matter, $\mathrm{d}f(W)/\mathrm{d}W$ is not identical to the (dipole transition) OOS related to the absorption of photons [17] (cf [12]); they are approximately equal if $\mathrm{Im}[-1/\epsilon(0, W)] \approx \mathrm{Im}[\epsilon(0, W)]$, i.e. if $|\epsilon(0, W)|^2 \approx 1$.

Experimental information on the OOS is presently available for many materials, mainly from optical and synchrotron radiation studies [18, 19] or as photoelectric absorption data [20, 21]. This information, complemented with assumptions about dispersion (i.e. variation of the GOS with Q), has been used to work out different GOS models [4–8]. We extend

the experimentally determined OOS, denoted $[\mathrm{d}f(W)/\mathrm{d}W]_{\mathrm{exp}}$, into the GOS (i.e. to values $Q > 0$) by

$$\frac{\mathrm{d}f(Q,W)}{\mathrm{d}W} = \int_0^\infty \left[\frac{\mathrm{d}f(W')}{\mathrm{d}W'}\right]_{\mathrm{exp}} F(W';Q,W)\,\mathrm{d}W' \tag{9}$$

where $F(W';Q,W)$ is the 'one-electron' GOS or extension algorithm, i.e. the GOS obtained by extending a unit strength (one-electron) optical oscillator with resonance energy W' into the $Q > 0$ region (see [9]). In fact, the true GOS can always be expressed in this way [9]. The approximation to be introduced consists basically of the use of phenomenological but physically motivated extension algorithms. Expressions for $F(W';Q,W)$ will be given below. Note that, as required by equation (9), $F(W';0,W) = \delta(W'-W)$.

2.2. *Preparation of the OOS*

The OOSs adopted in the present calculations have been obtained from optical data which are available either in the form of the refractive index n and the extinction coefficient κ [18, 19] or as the photoelectric cross section σ_{ph} [20, 21]. In the first case, the OOS is evaluated by using equation (4) for $Q = 0$ with $\epsilon = (n+\mathrm{i}\kappa)^2$. In the second case, the OOS is obtained by means of the relation [22]

$$\mathrm{d}f(W)/\mathrm{d}W = (mc/2\pi^2e^2\hbar)\sigma_{\mathrm{ph}} \tag{10}$$

which applies when $|\epsilon|^2$ is close to unity.

Unfortunately, for most materials, experimental optical data currently available extend over limited energy-loss ranges so that the complete OOS can only be obtained approximately by combining a variety of measured data (usually from different authors, obtained with various instruments and techniques and on different samples) with theoretical photoelectric cross sections. For the noble metals Cu and Au, we have constructed the 'experimental' OOS by combining optical data (i.e. refractive index and extinction coefficient) from [18] for $W < W_{\mathrm{od}}$, and theoretical photoelectric cross sections from Cullen *et al* [21] for $W > W_{\mathrm{od}}$, with $W_{\mathrm{od}} = 0.9$ keV for Cu and 2 keV for Au. In the case of Al, we have directly employed the dielectric constant given by Smith *et al* [23, 24], extrapolated for $W > 10$ keV. For the semiconductor Si we have made use of data given by Bichsel [25], which cover the whole energy range of interest. All these OOSs are given in tabular form; in the numerical evaluation of integrals involving the OOS we have used the continuous function obtained by linear interpolation on a log–log representation of the tabulated values. Figure 1 shows the OOSs for Al, Si, Cu and Au.

The consistency of the adopted OOSs can be checked by means of various sum rules. We utilize the f sum rule [17, 18]

$$\frac{1}{Z}\int_0^\infty \frac{\mathrm{d}f(W)}{\mathrm{d}W}\,\mathrm{d}W = 1 \tag{11}$$

and the perfect-screening sum rule [26, 27] (or ps sum) which, when written in terms of the OOS, takes the form

$$\frac{\Omega_{\mathrm{p}}^2}{Z}\int_0^\infty \frac{1}{W^2}\frac{\mathrm{d}f(W)}{\mathrm{d}W}\,\mathrm{d}W = 1. \tag{12}$$

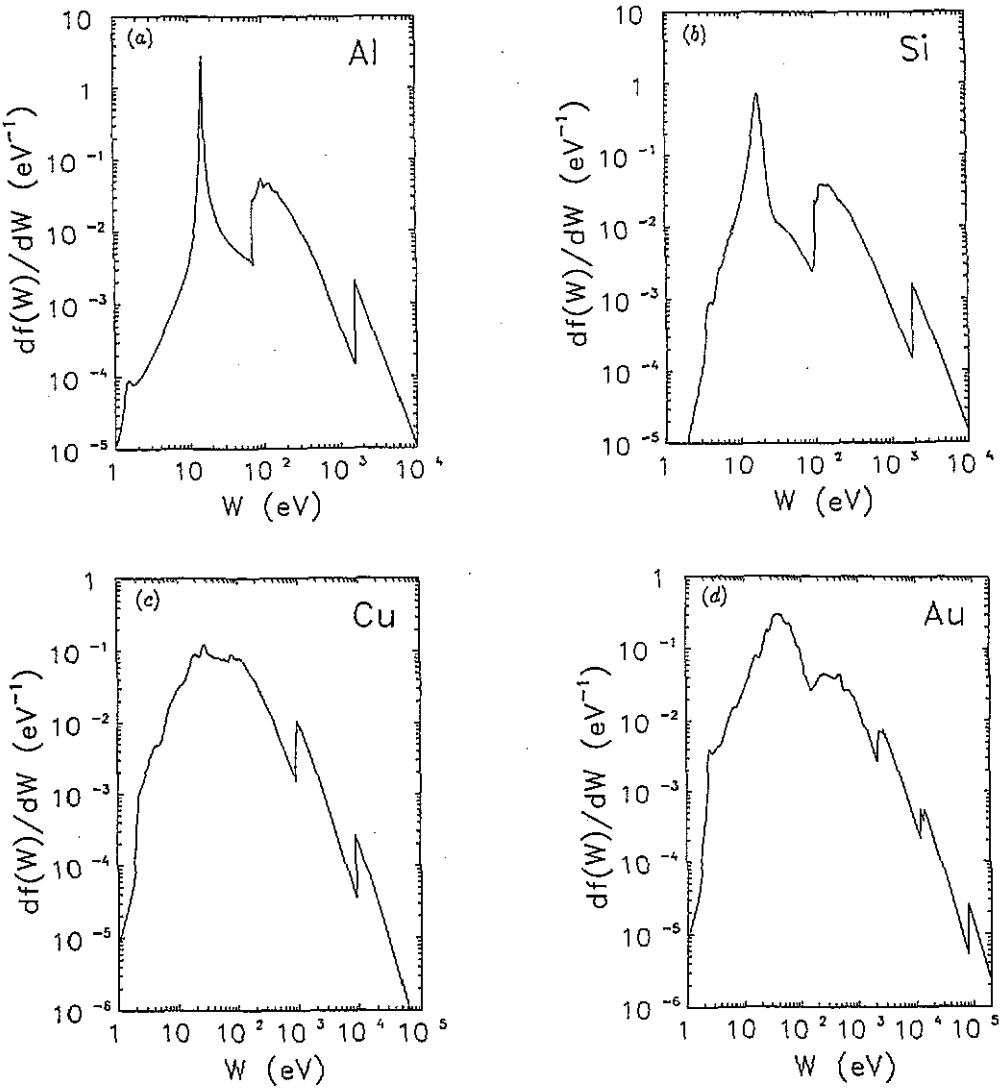

Figure 1. OOSS for (*a*) Al [23, 24], (*b*) Si [25] and for (*c*) Cu and (*d*) Au [18, 21].

The main contributions to the ps sum arise from the region of small energy losses and, therefore, this sum rule provides a check for the low energy loss behaviour of the OOS. The f sum rule is more sensitive to medium and large energy losses and, thus, it gives a global measure of the quality of the OOS in this region. Further relevant integrals of the OOS are

$$M_{\text{tot}}^2 \equiv \int_0^\infty \frac{R}{W} \frac{\mathrm{d}f(W)}{\mathrm{d}W} \mathrm{d}W \tag{13}$$

(where $R = 13.6$ eV is the Rydberg energy) and the well-known mean ionization energy I given by

$$\ln I \equiv \left(\int_0^\infty \frac{\mathrm{d}f(W)}{\mathrm{d}W} \mathrm{d}W \right)^{-1} \int_0^\infty \ln W \frac{\mathrm{d}f(W)}{\mathrm{d}W} \mathrm{d}W. \tag{14}$$

The values of the f and ps sums and the quantities M_{tot}^2 and I, computed from the OOSs described above, are given in table 1. The reliability of the OOSs for Al [23, 24] and Si [25] is supported by the values of the f and ps sums.

Table 1. Values of the f and ps sums, equations (11) and (12), the mean ionization energy I, equation (14), and M_{tot}^2, equation (13), for different materials. I_{SB} are the mean ionization energies recommended in [28].

Material	Z	f sum	ps sum	I (eV)	I_{SB} (eV)	M_{tot}^2
Al	13	0.993	0.984	164	166±2	3.08
Si	14	0.991	0.914	174	173±3	3.42
Cu	29	0.981	0.999	323	322±10	3.47
Au	79	0.968	1.090	737	790±30	6.38

From electron energy loss spectroscopy (EELS) measurements one can infer the energy loss spectrum in single inelastic collisions with scattering angle less than a certain value θ_{max}, determined by the experimental set-up. Usually, θ_{max} is small (a few degrees) and the initial kinetic energy is much larger than the observed energy losses. Under these circumstances ($\theta_{\mathrm{max}} \ll 1$, $W \ll E$), the EEL spectrum in single collisions can be computed, to lowest order, as

$$\left[\frac{\mathrm{d}\sigma}{\mathrm{d}W}\right]_{\theta<\theta_{\mathrm{max}}} = \int_{Q(\theta=0)}^{Q(\theta=\theta_{\mathrm{max}})} \frac{\mathrm{d}^2\sigma}{\mathrm{d}Q\mathrm{d}W}\,\mathrm{d}Q \approx \frac{\pi e^4}{E}\frac{1}{W}\frac{\mathrm{d}f(W)}{\mathrm{d}W}\ln\left[1+\left(\frac{2E\theta_{\mathrm{max}}}{W}\right)^2\right]. \tag{15}$$

This equation shows explicitly that, in this approximation, different extension algorithms lead to the same result; thus, the ability of a Monte Carlo program to reproduce such small-angle spectra is dependent primarily on the OOS. Small-angle EEL spectra for Cu, computed from the presently compiled OOS by means of equation (15) and derived from a measurement [29], are compared in figure 2.

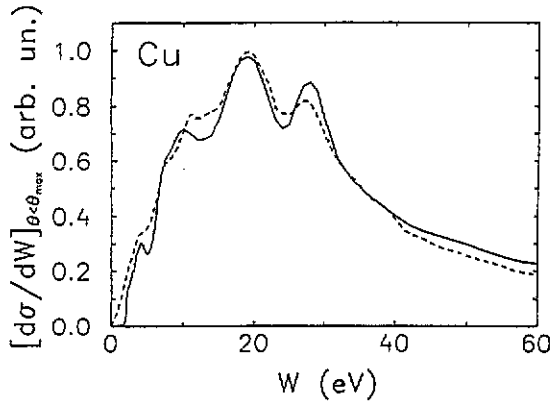

Figure 2. Single scattering EEL spectrum for electrons in Cu (E = 60 keV, θ_{max} = 0.1 rad), computed from the OOS by means of equation (15) (full curve) and obtained from experiment [29] (dashed curve).

2.3. Excitation of weakly bound electrons

FEG theory plays a central role in most of the optical-data models proposed to date. In the models proposed by Ashley [4–6] and Penn [7], the extension algorithms are provided either by the Lindhard theory or by suitable one-mode approximations to it. We may characterize the FEG by the plasmon energy $\mathcal{E}_p$, which is related to the electron gas density ρ through

$$\mathcal{E}_p = (4\pi\hbar^2 e^2 \rho/m)^{1/2}. \tag{16}$$

The one-electron GOS for a FEG with plasmon energy $\mathcal{E}_p$ is given by

$$F_L(\mathcal{E}_p; Q, W) = (2W/\pi\mathcal{E}_p^2)\mathrm{Im}\left(-1/\epsilon_L(\mathcal{E}_p; Q, W)\right) \tag{17}$$

where $\epsilon_L(Q, W)$ is the Lindhard dielectric function [3, 30]. It should be noticed that the OOS of equation (17) (neglecting plasmon damping) reduces to the delta function

$$F_L(\mathcal{E}_p; 0, W) = \delta(W - \mathcal{E}_p). \tag{18}$$

The evaluation of cross sections (7) for a FEG with the GOS given by equation (17) has to be performed numerically and is quite lengthy. To simplify the calculations, we use the following two-modes approximation (similar to the T model of reference [9]) for the one-electron GOS of the FEG:

$$F_T(\mathcal{E}_p; Q, W) \equiv [1 - g(Q)]\delta(W - W_r(Q)) + g(Q)\delta(W - Q) \tag{19}$$

where

$$W_r(Q) = \mathcal{E}_p + BQ \qquad g(Q) = \min\left\{1,\ A\frac{Q^3}{\mathcal{E}_p^2(\mathcal{E}_p + Q)}\right\}. \tag{20}$$

Equations (19) and (20) may be interpreted as follows. Within a limited region of small Q, two excitation modes coexist. One mode or branch with strength $1 - g(Q)$ corresponds to plasmon excitation with the dispersion relation $W_r(Q)$; the other, with strength $g(Q)$, represents electron–hole excitation. For large Q, the plasmon branch disappears and the electron–hole branch attains a unit strength. For small Q, $g(Q)$ decreases to zero roughly as Q^3; thus, the strength of the plasmon branch is unity for Q=0 [9].

The particular form of the functions $W_r(Q)$ and $g(Q)$ and the values of the parameters A and B have been determined by requiring the resulting one-electron cross sections to agree closely with those computed from the Lindhard dielectric function [31] (see below). The presently adopted values of these parameters are

$$A(\mathcal{E}_p) = \left(\frac{\chi^2}{3}\right)^{1/2}\left[\frac{1}{1 + \frac{2}{3}\chi^2} + \frac{1}{\chi(1 - \chi^2/3)^{1/2}}\tan^{-1}\left(\frac{(1 - \chi^2/3)^{1/2}}{\chi}\right)\right] \tag{21a}$$

for $\chi^2 < 3$,

$$A(\mathcal{E}_p) = \tfrac{2}{3} \tag{21b}$$

for $\chi^2 \geqslant 3$ and

$$B(\mathcal{E}_p) = (1 + \tfrac{1}{2}\chi)\tfrac{6}{5}\mathcal{E}_F/\mathcal{E}_p \tag{21c}$$

where

$$\mathcal{E}_F \equiv (\hbar^2/2m)\left(3\pi^2\rho\right)^{2/3} = \tfrac{1}{2}\left((9\pi^2/16)(\hbar/me^4)\right)^{1/3}\mathcal{E}_p^{4/3} \tag{22}$$

is the Fermi energy of the FEG and

$$\chi^2 \equiv \tfrac{3}{16}(\mathcal{E}_p/\mathcal{E}_F)^2. \tag{23}$$

(In the range $0 < \mathcal{E}_p < 100$ eV, A varies between $\frac{2}{3}$ and $\simeq 0.9$, and B between $\simeq 0.4$ and $\simeq 1.9$). Evidently, we have

$$\int_0^\infty F_T(\mathcal{E}_p; Q, W)\,dW = 1. \tag{24}$$

The mean free path and the stopping power of electrons moving in a FEG are given by $\lambda^{-1} = \rho\sigma^{(0)}$ and $S = \rho\sigma^{(1)}$, where $\sigma^{(n)}$ are the one-electron cross sections (7). However, the maximum energy loss is $W_{max} = E - \mathcal{E}_F$ since larger energy losses would place the incident electron into a state below the Fermi level. With the GOS given by equations (19)–(21) the cross sections (7) can be evaluated analytically.

The expression (21a) for the parameter A has been determined so as to exactly reproduce the analytical expressions obtained for the mean free path and the stopping power from Lindhard's theory in the low-energy limit [30, 31]. According to the Lindhard theory, the plasmon dispersion is given by $W_r(Q) = \mathcal{E}_p + 6\mathcal{E}_F Q/(5\mathcal{E}_p) + O(Q^2)$. The slope B of the plasmon line in the two-modes model, given by equation (21c), has been determined to optimize the agreement of the computed mean free paths and stopping powers with the results of Lindhard's theory.

Inverse mean free paths and stopping powers of electrons in electron gases of different plasmon energies, computed from Lindhard's GOS, equation (17), and from the two-modes model, equations (19)–(21), are compared in figure 3. It is seen that the two-modes model yields results which agree closely with those from the Lindhard theory.

The GOS obtained purely from the two-modes model is

$$\frac{df(Q,W)}{dW} = \int_0^\infty \left[\frac{df(W')}{dW'}\right]_{exp} F_T(W'; Q, W)\,dW' \tag{25}$$

where $F_T(W'; Q, W)$ is the one-electron GOS of a FEG with plasmon energy W' as defined in equation (19). (Replacing F_T by F_L in equation (25) we recover Penn's model [7].) Owing to equation (18) (or the first term in equation (19)), the GOS (25) reduces to the experimental OOS in the limit Q=0. Furthermore, by equation (24), the Bethe sum rule (3) is automatically satisfied, provided the adopted OOS fulfils the f sum rule. It may be noted that a continuous superposition of undamped FEG extension functions with varying W' apparently can be used to model, for example, short-lived (broad) plasmon excitations.

We expect extension models based on FEG theory to be sufficiently adequate for weakly bound electrons in general, i.e. also for non-conduction bands. Our arguments for this are briefly discussed in the appendix.

2.4. Excitation of inner-shell electrons

Models based on the FEG have been shown [8] to be unsuitable for describing inner-shell ionization. They permit energy losses less than the ionization threshold. Moreover, the

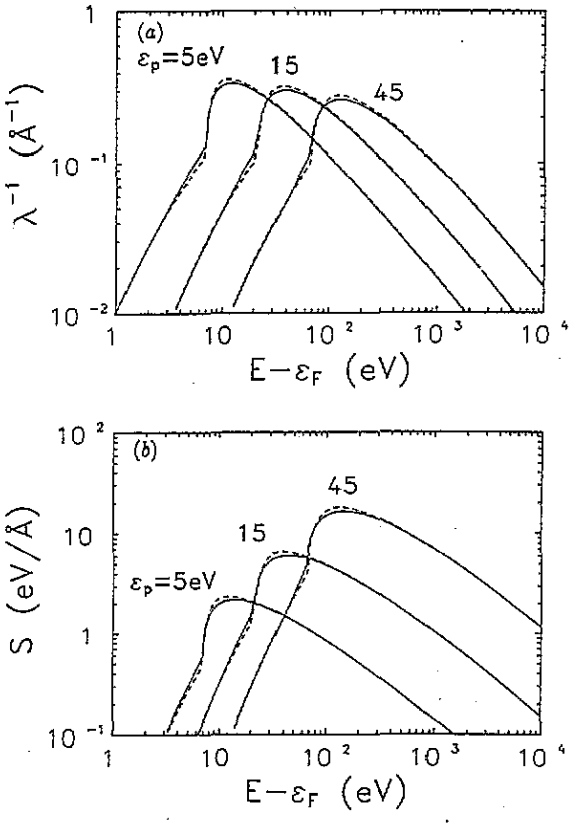

Figure 3. Inelastic inverse mean free path λ^{-1} (*a*) and stopping power S (*b*) for electrons in free-electron gases with $\mathcal{E}_p$ = 5, 15 and 45 eV. Full curves represent the results from Lindhard's theory; short-dashed curves have been obtained from the two-modes model given by equation (19).

plasmon branch gives rise to a pseudo-threshold, which however is displaced, because $B > 0$ (equation (20)). A GOS model which is more adequate for inner-shell ionization [8] may be expressed as

$$\frac{\mathrm{d}f(Q,W)}{\mathrm{d}W} = \int_0^\infty \left[\frac{\mathrm{d}f(W')}{\mathrm{d}W'}\right]_{\mathrm{exp}} F_\delta(W';Q,W)\,\mathrm{d}W' \tag{26}$$

where

$$F_\delta(W';Q,W) \equiv \delta(W-W')\,\Theta(W'-Q) + \delta(W-Q)\,\Theta(Q-W') \tag{27}$$

and Θ is the unit step function. The one-electron GOS defined by equation (27) will be referred to as a 'δ-oscillator' [32] (the S model of reference [9]). In this dispersion relation between Q and W, the first term models the contribution from 'distant' collisions (i.e. dipole transitions in the optical limit), while the second term models the contribution from 'close' collisions (i.e. the Bethe ridge) [9, 32]. K-shell ionization cross sections computed from the GOS model given by equation (26), using hydrogenic OOSs, are in good agreement with experimental data [8].

2.5. New optical-data model

2.5.1. Extension formula. We have previously compared different optical-data GOS models and suggested that a combination of the two-modes model given by equation (19) (for

valence electron excitations) and the δ-oscillator model given by equation (27) (for core electron excitations) should be a convenient approach [9]. Accordingly, we shall compute the GOS from equation (9) with

$$F(W';Q,W)=\begin{cases}F_{\mathrm{T}}(W';Q,W) & \text{if } W'<W_{\mathrm{s}}\\ F_{\delta}(W';Q,W) & \text{if } W'>W_{\mathrm{s}}.\end{cases} \tag{28}$$

The switch energy W_{s} separates the region of low resonance energies W', where the excitations in the low-Q limit have a large degree of collective character, from the high resonance energy region. W_{s} is placed at the first threshold for inner-shell excitation, i.e. at the smallest core-level binding energy (see table 2). The regions $W'<W_{\mathrm{s}}$ and $W'>W_{\mathrm{s}}$ are thus characterized by different dispersion relations.

Table 2. Fermi energy E_{F}, switch energy W_{s} and correspondig core level for different materials. For Si, we have assumed four valence electrons per atom, treating them as a FEG [25].

Material	E_{F} (eV)	W_{s} (eV)	level
Al	11.7	73	2p
Si	12.5	99	2p
Cu	7.0	74	3p
Au	5.5	54	$5p_{3/2}$

The DCS given by equation (1) can be written as

$$\frac{\mathrm{d}^2\sigma}{\mathrm{d}Q\mathrm{d}W}=\int_0^{\infty}\left[\frac{\mathrm{d}f(W')}{\mathrm{d}W'}\right]_{\mathrm{exp}}\frac{\mathrm{d}^2\sigma_1(W')}{\mathrm{d}Q\mathrm{d}W}\,\mathrm{d}W' \tag{29}$$

where

$$\mathrm{d}^2\sigma_1(W')/\mathrm{d}Q\mathrm{d}W=(\pi e^4/E)(1/WQ)F(W';Q,W) \tag{30}$$

may be regarded as the DCS for a one-electron oscillator with resonance energy W' in the OOS limit.

2.5.2. Exchange correction. When the projectile is an electron, exchange between the incident electron and the electrons in the medium must be taken into account. To our knowledge, exchange effects in optical-data model calculations have only been considered by Ashley [5, 6], who used a heuristic approach. A more conventional tool for dealing with exchange effects is provided by the Ochkur approximation [10]. The Born–Ochkur DCS is given by

$$\mathrm{d}^2\sigma/\mathrm{d}Q\mathrm{d}W=(\pi e^4/E)(1/WQ)\left[1-Q/E+(Q/E)^2\right]\mathrm{d}f(Q,W)/\mathrm{d}W \tag{31}$$

and is obtained by considering that the exchange scattering amplitude is approximately given by the leading term of an expansion of the Born–Oppenheimer amplitude in inverse powers of E [11]. Therefore, the Born–Ochkur approximation is essentially a high-energy approximation. For energies near the ionization thresholds, where optically allowed excitations (i.e. excitations with $Q \ll W$) dominate, the Born–Ochkur approximation gives a satisfactory description of exchange effects [33]. On the other hand, collisions with energy

loss W much larger than the energies of the electrons in the target can be described as binary collisions with free electrons at rest. The DCS for this kind of collision may be calculated exactly [13] and, for projectiles with kinetic energy much larger than the Rydberg energy, it simplifies to the non-relativistic Møller DCS

$$\frac{\mathrm{d}\sigma}{\mathrm{d}W} = \frac{\pi e^4}{E}\frac{1}{W^2}\left[1 - \frac{W}{E-W} + \left(\frac{W}{E-W}\right)^2\right]. \tag{32}$$

Clearly, this result differs from the limiting behaviour of the Ochkur exchange correction for large W.

We shall introduce exchange effects by using the following one-electron DCS:

$$\frac{\mathrm{d}^2\sigma_1(W')}{\mathrm{d}Q\mathrm{d}W} = \frac{\pi e^4}{E}\frac{1}{WQ}\left[1 - \frac{Q}{E+W'-W} + \left(\frac{Q}{E+W'-W}\right)^2\right]F(W';Q,W). \tag{33}$$

The modification introduced here, which is permissible owing to the asymptotic nature of the Born–Ochkur approximation, agrees with the usual correction given in equation (31) when $W=W'$ and has the desirable effect of leading to the non-relativistic Møller DCS, equation (32), when $W \gg W'$ (since then $Q \simeq W$). Due to the indistinguishability of the 'primary' and the 'struck' electrons, we can consider the primary as the most energetic after the collision. Owing to this convention, in collisions with free electrons at rest the energy loss of the primary electron cannot exceed the value $W_{\max} = \frac{1}{2}E$. In the case of inner-shell ionization, the primary and secondary electrons have the same kinetic energy when $W = W_{\max} = \frac{1}{2}(E + E_b)$, where E_b is the ionization energy of the considered shell. Notice that, by using this value for $W_{\max}$, the Ochkur correction keeps the ionization threshold unaltered.

The value of the maximum energy loss is also limited by the exclusion principle, which forbids energy losses larger than $E - E_F$ that would place the incident electron into an occupied state below the Fermi level E_F of the medium (see table 2).

2.5.3. Resulting one-electron cross sections. The exchange corrected one-electron DCSs for $W' > W_s$, i.e. when the extension algorithm is the δ-oscillator given by equation (27), are computed as

$$\begin{aligned}\frac{\mathrm{d}^2\sigma_1(W')}{\mathrm{d}Q\mathrm{d}W} = {} & \frac{\pi e^4}{E}\frac{1}{WQ}\left[1 - \frac{Q}{E} + \left(\frac{Q}{E}\right)^2\right]\delta(W-W')\Theta(W'-Q) \\ & + \frac{\pi e^4}{E}\frac{1}{WQ}\left[1 - \frac{Q}{E+W'-W} + \left(\frac{Q}{E+W'-W}\right)^2\right] \\ & \times \delta(W-Q)\Theta(Q-W').\end{aligned} \tag{34}$$

The first term in this expression corresponds to distant ('resonance') collisions; the Ochkur correction factor has the usual form given by equation (31). The second term accounts for close (binary) collisions; when $W' \ll E - W$, it reduces to the non-relativistic Møller DCS, equation (32).

In order to get a general recipe which keeps the ionization thresholds unaltered, the maximum energy loss is taken to be $W_{\max}(W') = \min\{E - E_F, \frac{1}{2}(E + W')\}$. This is equivalent to considering W' as the 'binding energy' of the target electron. This assumption

was also adopted by Ashley [5] and is justified by the fact that most inner-shell excitations occur for W' not much larger than the ionization threshold.

Excitations with $W' < W_s$ are treated as if they occur in a FEG with plasmon energy W', and are described by using the two-modes GOS model given by (19). Since the Ochkur exchange correction is based on the assumption of single-electron excitations, it is not justified for plasmon (i.e. collective) excitations of an electron gas. Therefore, the one-electron DCSs for $W' < W_s$ are split into contributions from electron–hole and plasmon-like excitations:

$$d^2\sigma_1(W')/dQdW = d^2\sigma_{1,eh}(W')/dQdW + d^2\sigma_{1,pl}(W')/dQdW. \tag{35}$$

The contribution from electron–hole excitations, including Ochkur's exchange correction, is given by (see equations (19) and (33))

$$\frac{d^2\sigma_{1,eh}(W')}{dQdW} = \frac{\pi e^4}{E}\frac{1}{WQ}\left[1 - \frac{Q}{E-W} + \left(\frac{Q}{E-W}\right)^2\right] g(Q)\delta(W-Q). \tag{36}$$

Here the maximum energy loss is taken to be $W_{max}(W') = \min\{E - E_F, \frac{1}{2}E\}$, i.e. the 'binding energy' is set equal to zero. The one-electron DCS for plasmon-like excitations is computed directly from equations (19) and (30), i.e.

$$d^2\sigma_{1,pl}(W')/dQdW = (\pi e^4/E)\,(1/WQ)\,[1 - g(Q)]\,\delta(W - W_r(Q)) \tag{37}$$

and the maximum energy loss is $W_{max}(W') = E - E_F$.

Finally, to obtain the inelastic mean free path λ and the stopping power S we have to compute the integrals

$$\sigma^{(n)} \equiv \int_0^\infty \left[\frac{df(W')}{dW'}\right]_{exp} \sigma_1^{(n)}(W')\,dW' \tag{38}$$

for $n = 0$ and $n = 1$, respectively, where

$$\sigma_1^{(n)}(W') = \int_0^{W_{max}(W')} dW\, W^n \int_{Q_-}^{Q_+} dQ\, \frac{d^2\sigma_1(W')}{dQdW} \tag{39}$$

are the one-electron total cross sections which, by using equations (34)–(37), can be evaluated analytically. The resulting expressions are lengthy, but simple to code in a computer program [34]. The numerical evaluation of λ and S reduces to a single quadrature.

3. Calculation of λ and S

Computed inelastic mean free paths and stopping powers for Al, Si, Cu and Au are shown in figures 4–7 as functions of $E - E_F$. For comparison purposes, we also give the results from the optical-data model calculations of Ashley [6] and of Tanuma *et al* [35]. These authors used OOSs and extension algorithms different from the ones adopted here. Ashley used a different approach to introduce exchange effects, which are neglected in the calculations on mean free paths by Tanuma *et al*. The magnitude of the exchange corrections on calculated λ and S is indicated in figure 5. Exchange effects have a stronger influence on the stopping power than on the mean free path (since S is more sensitive to the high energy loss part of the inelastic DCS). The effect of the value of W_s on λ and S is indicated in figure 7, where we compare results obtained with $W_s = 30$, 54 and 80 eV for Au. The dependence on W_s can be understood from the global analysis in [9].

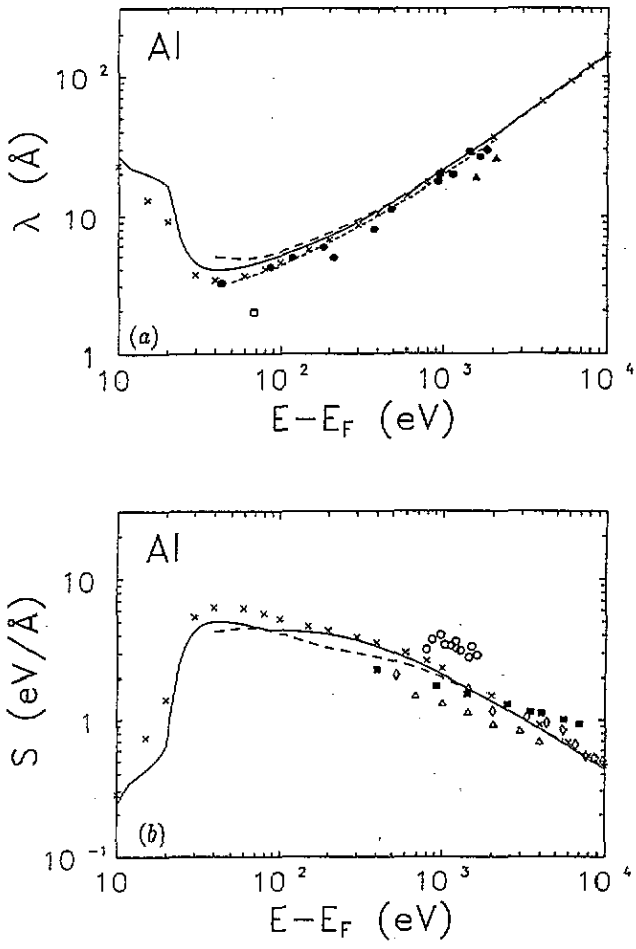

Figure 4. Inelastic mean free path λ (*a*) and stopping power S (*b*) for electrons in Al. Results from the present optical-data model are represented as full curves. Short-dashed and long-dashed curves represent the optical-data model calculations of Tanuma *et al* [35] and of Ashley [6], respectively. Crosses are theoretical calculations of Ashley *et al* [16]. Experimental data for λ are from references [36] (●), [37] (□) and [38] (▲); experimental data for S are from references [39] (◇), [40] (○), [41] (■) and [42] (△).

4. Fitted analytical formulae for λ and S

For practical purposes, it may be useful to have simple analytical formulae for the inelastic mean free path and the stopping power. We use the asymptotic formulae due to Bethe [12] as a guide to obtain expressions with a wider range of validity. The Bethe formula for the mean free path is

$$\lambda^{-1} = N(\pi e^4/ER)\left[M_{\rm tot}^2 \ln(4c_{\rm tot}E/R) + \gamma_{\rm tot}(R/E) + {\rm O}[(R/E)^2]\right]. \tag{40}$$

The quantities $c_{\rm tot}$ and $\gamma_{\rm tot}$ are integral properties of the GOS, which cannot be computed only from the OOS.

The Bethe formula for the stopping power can be written

$$S = N(2\pi e^4/E)Z\left[\ln(E/I) + \tfrac{1}{2}(1 - \ln 2) + {\rm O}(R/E)\right] \tag{41}$$

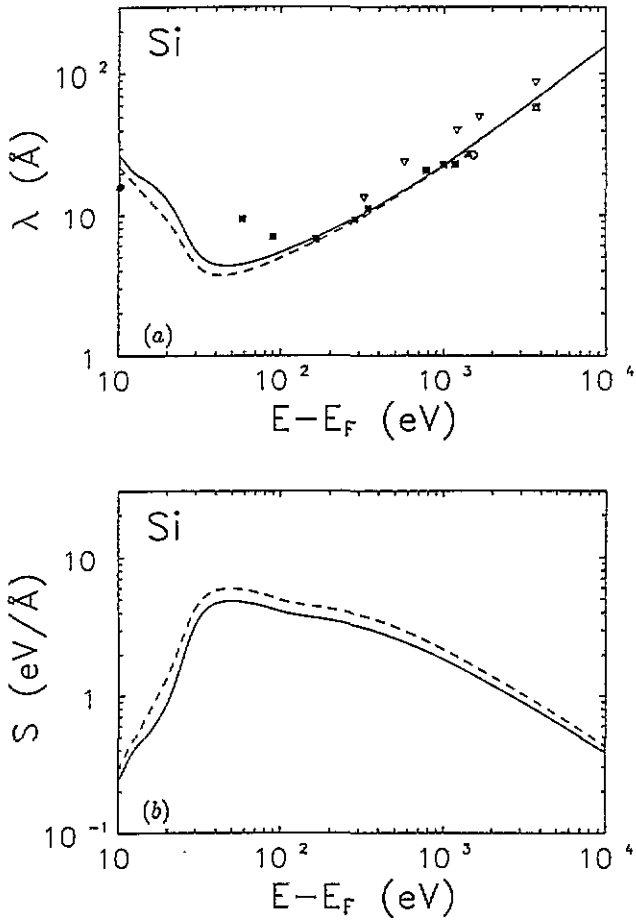

Figure 5. Inelastic mean free path λ (*a*) and stopping power S (*b*) for electrons in Si. Results from the present optical-data model are represented as full curves. Results obtained by excluding the Ochkur exchange correction are represented as dashed curves. Experimental data for λ are from references [43] (○), [44] (●), [45] (△), [46] (▲), [47] (□), [48] (■) and [49] (▽).

where I is the mean ionization energy. The second term on the right-hand side of equation (41) originates from exchange.

From formulae (40) and (41) we expect that, for energies which are not too low, the calculated mean free paths and stopping powers may be closely reproduced by the following expressions:

$$\lambda^{-1} = N(\pi e^4/ER)\left[M_{\text{tot}}^2 \ln(4a_1 E/R) + a_2(R/E) + a_3(R/E)^2\right] \tag{42}$$

$$S = N(2\pi e^4/E)Z\left[\ln(E/I) + \tfrac{1}{2}(1-\ln 2) + a_4(R/E) + a_5(R/E)^2\right] \tag{43}$$

where the dimensionless quantities $a_1, \ldots, a_5$ are considered as adjustable parameters.

Except for small kinetic energies, the results obtained by our optical-data model calculation can be closely approximated by expressions (42) and (43). The values of the parameters $a_1, \ldots, a_5$, given in table 3, have been determined by numerical least squares fit to the calculated mean free path and stopping power for kinetic energies larger than

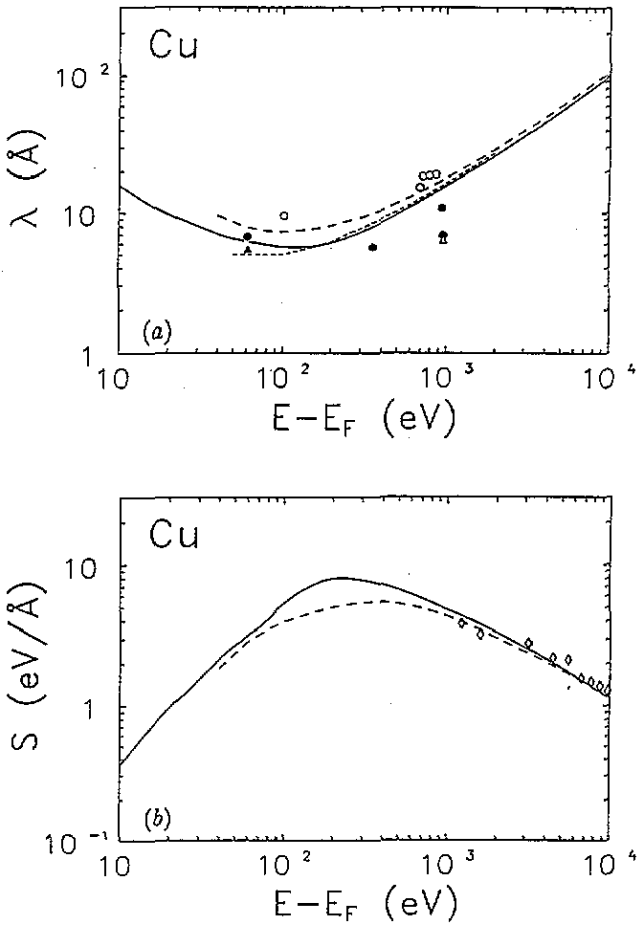

Figure 6. Inelastic mean free path λ (*a*) and stopping power *S* (*b*) for electrons in Cu. Results from the present optical-data model are represented as full curves. Short-dashed and long-dashed curves represent the optical-data model calculations of Tanuma *et al* [35] and of Ashley [6], respectively. Experimental data for λ are from references [43] (●), [50] (△), [51] (○) and [52] (▲); experimental data for *S* are from reference [39] (◇).

300 eV for λ and larger than $Z \times 10$ eV for *S*. It is not convenient to extend the fit to lower energies, since in this region the behaviour of λ and *S* cannot be reproduced by the simple expressions (42) and (43). In the considered energy intervals, the relative differences between the numerical values and the fitted analytical formulae are less than 2%.

Table 3. Parameters of the analytical formulae (42) and (43) for different materials.

Material	a_1	a_2	a_3	a_4	a_5
Al	0.8532	−65.37	638.0	7.896	−19.17
Si	0.8503	−70.35	685.8	8.666	−21.62
Cu	0.4504	−103.4	1114	18.92	−98.98
Au	0.4009	−204.4	2421	52.93	−798.3

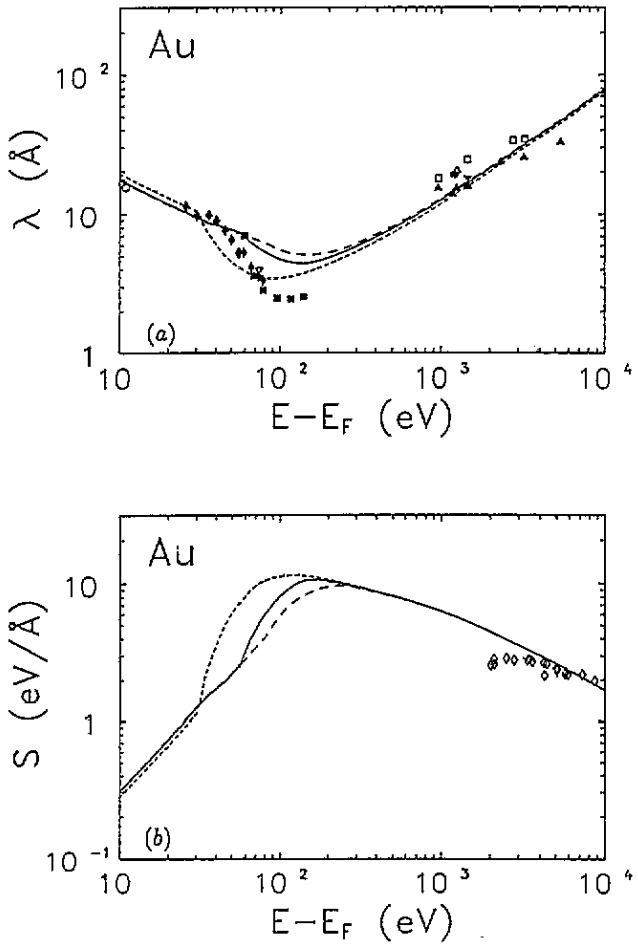

Figure 7. Inelastic mean free path λ (*a*) and stopping power S (*b*) for electrons in Au. Results obtained from the present optical-data model with W_s = 30, 54 and 80 eV are represented as short-dashed, full and long-dashed curves, respectively. Experimental data for λ are from references [50] (▽), [53] (○), [54] (▲), [55] (□), [56] (■), [57] (▼), [58] (◇), [59] (△) and [60] (●); experimental data for S are from reference [39] (◇).

Appendix 1.

The application of FEG theory as an extension algorithm for the contribution to the OOS from electrons in non-conduction bands—for example the valence electrons in Si and the 3d electrons in Cu—may be questioned. As available one-electron excitations are interband rather than intraband transitions, the FEG model is apparently in error since it allows energy losses below the energy gap threshold. A basic argument in favour of the FEG model is the importance of collective effects in the excitation of weakly bound electrons in condensed matter [14]. For example, it would not be possible to separate the OOS into different regions originating from the 4s and the 3d electrons in Cu, due to their mutual polarization. Due to this collective behaviour, one might expect a similar dispersion relation as in the FEG.

Several authors have presented models for the interaction of a charged particle with a semiconductor or insulator by introducing a band gap in a FEG model (see e.g. references

[61–63]). In this spirit, we have examined the effect of a 'band gap' introduced into the two-modes model. For brevity and clearness we neglect exchange and consider a simplified two-modes model of the FEG with the GOS:

$$F(\mathcal{E}_p; Q, W) = [1 - g(Q)]\delta(W - (\mathcal{E}_p + Q)) + g(Q)\delta(W - Q) \tag{A.1}$$

where

$$g(Q) = \min\{1, Q^3/\mathcal{E}_p^3\}. \tag{A.2}$$

A band gap E_g is introduced (preserving the validity of the sum rule (3) and algebraic simplicity) by changing equation (A.1) into

$$F(\mathcal{E}_p; Q, W) = [1 - g(Q)]\delta(W - (\mathcal{E}_p + Q)) + g(Q)\delta(W - \max\{E_g, Q\}). \tag{A.3}$$

For incident electron energies $E < E_g$, the cross sections obtained with equation (A.3) will be zero. For $E > E_g$, the results of equations (A.1) and (A.3) will differ only in the contribution from the second term in the interval $0 < Q < E_g$. A simple calculation shows that the differences in mean free path and stopping power between (A.1) and (A.3) are negligible, except at energies $E < 2E_g$. Since E_g typically has a magnitude of a few eV, this difference can be ignored at energies of interest. Moreover, 'false' energy losses $W < E_g$ are rare since they appear only for $Q < E_g$, where the plasmon mode nearly exhausts the Bethe sum rule. Evidently, they do not appear in the small-angle spectrum, as seen from equation (15). We conclude that the FEG should be an acceptable approximation.

Acknowledgments

We are indebted to Dr Hans Bichsel for providing the OOS for Si in numerical form and to Josep Baró for computational assistance. Financial support from the Comisión para la Investigación Científica y Técnica (Spain), Project no. PB90-0446, is gratefully acknowledged. D Liljequist wishes to express his gratitude to the University of Stockholm and the Granholm Foundation for a travel grant.

References

[1] Tung C J, Ashley J C and Ritchie R H 1979 *Surf. Sci.* **81** 427
[2] Lindhard J and Scharff M 1953 *K. Danske Vidensk. Selsk. Mat.-Fys. Meddr.* **27** 1
[3] Lindhard J 1954 *K. Danske Vidensk. Selsk. Mat.-Fys. Meddr.* **28** 1
[4] Ashley J C 1982 *J. Electr. Spectrosc. Relat. Phenom.* **28** 177
[5] Ashley J C 1988 *J. Electr. Spectrosc. Relat. Phenom.* **46** 199
[6] Ashley J C 1989 *Oak Ridge National Laboratory Report* CONF-8909210
[7] Penn D R 1987 *Phys. Rev.* B **35** 482
[8] Mayol R and Salvat F 1990 *J. Phys. B: At. Mol. Opt. Phys.* **23** 2117
[9] Fernández-Varea J M, Mayol R, Salvat F and Liljequist D 1992 *J. Phys.: Condens. Matter* **4** 2879
[10] Ochkur V I 1964 *Sov. Phys.-JETP* **18** 503
[11] Bransden B H 1983 *Atomic Collision Theory* 2nd edn (Reading, MA: Benjamin Cummings)
[12] Inokuti M 1971 *Rev. Mod. Phys.* **43** 297
[13] Mott N F and Massey H S W 1965 *Theory of Atomic Collisions* 3rd edn (Oxford: Clarendon)
[14] Fano U 1956 *Phys. Rev.* **103** 1202
[15] Leapman R D, Rez P and Mayers D F 1980 *J. Chem. Phys.* **72** 1232

[16] Ashley J C, Tung C J and Ritchie R H 1979 *Surf. Sci.* **81** 409
[17] Bransden B H and Joachain C J 1983 *Physics of Atoms and Molecules* (London: Longman)
[18] Palik D (ed) 1985 *Handbook of Optical Constants of Solids* (New York: Academic)
[19] Hagemann H-J, Gudat W and Kunz C 1974 *Deutsches Elektronen-Synchrotron Report SR-74/7* (Hamburg)
[20] Henke B L, Lee P, Tanaka T J, Shimabukuro R L and Fujikawa B K 1982 *At. Data Nucl. Data Tables* **27** 1
[21] Cullen D E, Chen M H, Hubbell J H, Perkins S T, Plechaty E F, Rathkopf J A and Scofield J H 1989 *Lawrence Livermore National Laboratory UCRL-50400* vol 6, parts A and B
[22] Fano U and Cooper J W 1968 *Rev. Mod. Phys.* **40** 441
[23] Smith D Y, Shiles E and Inokuti M in reference [18], pp 369–406
[24] Shiles E, Sasaki T, Inokuti M and Smith D Y 1980 *Phys. Rev.* B **22** 1612
[25] Bichsel H 1988 *Rev. Mod. Phys.* **60** 663
[26] Pines D and Nozières P 1989 *The Theory of Quantum Liquids: Normal Fermi Liquids* (Redwood City, CA: Addison-Wesley)
[27] Mahan G D 1983 *Many-Particle Physics* (New York: Plenum)
[28] Seltzer S M and Berger M J 1982 *National Bureau of Standards Report No. NBSIR 82-2572*
[29] Misell D L and Atkins A J 1973 *Phil. Mag.* **27** 95
[30] Ritchie R H 1957 *Phys. Rev.* **106** 874
[31] Lindhard J and Winter A 1964 *K. Danske Vidensk. Selsk. Mat.-Fys. Meddr.* **34** 1
[32] Liljequist D 1985 *J. Appl. Phys.* **57** 657
[33] Hippler R 1990 *Phys. Lett.* **144A** 81
[34] Complete evaluation formulae and FORTRAN source program are provided in: Fernández-Varea J M, Liljequist D, Mayol R and Salvat F 1992 *University of Stockholm Institute of Physics Report 92–06*
[35] Tanuma S, Powell C J and Penn D R 1991 *Surf. Interface Anal.* **17** 911
[36] Tracy J C 1974 *J. Vac. Sci. Technol.* **11** 280
[37] Powell C J, Stein R J, Needham Jr P B and Driscoll T J 1977 *Phys. Rev.* B **16** 1370
[38] Kanter H 1970 *Phys. Rev.* B **1** 2357
[39] Al-Ahmad K O and Watt D E 1983 *J. Phys. D: Appl. Phys.* **16** 2257
[40] Garber F W, Harter J A, Birkhoff R D and Ritchie R H 1969 *Oak Ridge National Laboratory Report* ORNL-TM-2406
[41] Young J R 1956 *Phys. Rev.* **103** 292
[42] Fitting H-J 1974 *Phys. Status Solidi* a **26** 525
[43] Seah M P 1972 *Surf. Sci.* **32** 703
[44] Pierce D T and Spicer W E 1972 *Phys. Rev.* B **5** 3017
[45] Ishizaka A, Iwata S and Kamagaki Y 1979 *Surf. Sci.* **84** 355
[46] Hill J M, Royce D G, Fadley C S, Wagner L F and Grunthaner F G 1976 *Chem. Phys. Lett.* **44** 225
[47] Flitsch R and Raider S I 1975 *J. Vac. Sci. Technol.* **12** 305
[48] Zaporozhchenko V I, Kalafati Yu D, Kukharenko Yu A and Sergeev V M 1979 *Izv. Akad. Nauk SSSR, Ser. Fiz.* **43** 1919
[49] Klasson M, Berndtsson A, Hedman J, Nilsson R, Nyholm R and Nordling C 1974 *J. Electr. Spectrosc. Relat. Phenom.* **3** 427
[50] Palmberg P W and Rhodin T N 1968 *J. Appl. Phys.* **39** 2425
[51] Burke M A and Schreurs J J 1982 *Surf. Interface Anal.* **4** 42
[52] Seah M P 1973 *J. Phys. F: Met. Phys.* **3** 1538
[53] Kanter H 1970 *Phys. Rev.* B **1** 522
[54] Brunner J and Zogg H 1974 *J. Electr. Spectrosc. Relat. Phenom.* **5** 911
[55] Klasson M, Hedman J, Berndtsson A, Nilsson R and Nordling C 1972 *Phys. Scr.* **5** 93
[56] Norman D and Woodruff D P 1977 *Solid State Commun.* **22** 711
[57] Henke B L 1972 *Phys. Rev.* A **6** 94
[58] Lindau I, Pianetta P, Yu K Y and Spicer W E 1976 *J. Electr. Spectrosc. Relat. Phenom.* **8** 487
[59] Baer Y, Heden P F, Hedman J, Klasson M and Nordling C 1970 *Solid State Commun.* **8** 1479
[60] Cadman P, Evans S, Scott J D and Thomas J M 1970 *J. Chem. Soc. Faraday Trans. II* **71** 1777
[61] Brandt W and Reinheimer J 1970 *Phys. Rev.* B **2** 3104
[62] Emerson L C, Birkhoff R D, Anderson V E and Ritchie R H 1973 *Phys. Rev.* B **7** 1798
[63] Levine Z H and Louie S G 1982 *Phys. Rev.* B **25** 6310